Supplemental materials

Bialucha et al., http://www.jcb.org/cgi/content/full/jcb.200612022/DC1

Results

Determination of the binding site of p32 and mLgl2

To determine the p32 binding site on mLgl2, we generated N-terminal (mLgl2N) and C-terminal (mLgl2C) constructs of mLgl2 (Fig. S1 D, schematic). p32 bound to both full-length mLgl2 and mLgl2C, but not to mLgl2N, indicating that the site of interaction resides within amino acids 544–1027 of mLgl2 (Fig. S1 D). Immunoprecipitations of p32 with further truncations of the mLgl2 C terminus showed specific binding of p32 to a fragment of mLgl2 (mLgl2C1) that includes the highly conserved regulatory phosphorylation sites of mLgl2 (Fig. S1 E). However, the interaction of p32 with mLgl2C1 was weaker than that with full-length mLgl2, suggesting the involvement of other regions of mLgl2 in the interaction.

It has been shown that 73 amino acids of the N terminus of p32 are cleaved off to form the mature protein, which contains three α helices. Two α helices at the C terminus are highly conserved between different species (Fig. S1 F, bottom schematic). To determine the mLgl2 binding site on p32, we generated GFP-tagged fusion proteins of the full-length (p32FL), N terminus (p32N) and C terminus (p32C) of p32. Immunoprecipitation experiments revealed that mLgl2-WT bound to p32FL and p32C, but not to p32N (Fig. S1 F).

Materials and methods

Plasmids

To construct pcDNA-FLAG-mLgl2-WT, the cDNA encoding the N terminus of mLgl2 (amino acids 1–389) was amplified by PCR using a mouse mLgl2 EST clone (IMAGE clone 4936023; RZPD Deutsches Ressourcenzentrum für Genomforschung GmbH) and ligated into the EcoRI–NotI sites of pcDNA-FLAG-1Ab. Then, the cDNA encoding the remaining C terminus of mLgl2 was excised from the EST clone and sequentially ligated into the NheI–NotI sites of the above construct. pcDNA-FLAG-mLgl2-SA and -SD were generated from pcDNA-FLAG-mLgl2-WT using the QuikChange Site-Directed Mutagenesis kit (Stratagene). The following primers were used: 5′-CTGTCTCGAGTAAAGGCCCTCAAGAAGGCTCTACGTCAGGCATTCCGT CGGATGCGTC-3′ and 5′-GACGCATCCGACGGAATGCCTGACGTAGAGCCTT CTTGAGGGCCTTTACTCGAGACAG-3′ for SA and 5′-CTGTCTCGAGTC AAGGACCTCAAGAAGGATCTACGTCAGGACTTCCGTCGGATGCGTC-3′ and 5′-GACGCATCCGACGGAAGTCCTGACGTAGATCCTTCTTGAGGTCCTTT ACTCGAGACA-3′ for SD, respectively. These mutations changed serines 645, 649, and 653 to alanine (SA) and aspartic acid (SD), respectively. To produce pEGFP- and pMAL-mLgl2 constructs, the cDNAs of mLgl2-WT, -SA, or -SD were excised from the respective pcDNA-FLAG constructs and ligated into the XhoI site of pEGFP-C2 (CLONTECH Laboratories, Inc.) or EcoRI site of pMAL (New England Biolabs, Inc.), respectively. To generate mLgl2N and mLgl2C, pcDNA-FLAG-mLgl2-WT was digested with EagI–NotI, and the excised cDNA was ligated into the NotI site of pcDNA-FLAG-2Ab to produce pcDNA-FLAG-mLgl2C, whereas the remaining vector was religated to produce pcDNA-FLAG-mLgl2N. The cDNA of mLgl2C was further cleaved by PstI into fragments and ligated into pcDNA-FLAG to produce pcDNA-FLAG-mLgl2C1, -C2, and -C3 constructs. pEGFP-p32FL was constructed by PCR using a human EST clone (IMAGE clone 5493107; Geneservice Ltd.) and ligation into the EcoRI–BamHI sites of pEGFP-C1. pRK5Myc-p32 and pQE-His-p32 were made from pEGFP-p32FL by ligation into the BamHI sites of pRK-5Myc and pQE30 (QIAGEN), respectively. pEGFP-p32-N and -C were generated using PCR and insertion in the EcoRI–BamHI sites of pEGFP-C1. pEGFP-p32 (p32-GFP) was produced by PCR using the above EST clone and ligation into the BamHI–EcoRI sites of pEGFP-N1. To construct pcDNA4/TO/p32-GFP, the p32 cDNA linked to GFP from pEGFP-p32 was inserted into the EcoRI–NotI sites of pcDNA4/TO (Invitrogen). pEGFP-PKCζ was constructed by PCR using a human PKCζ EST clone (IMAGE clone 2987996; Geneservice Ltd.) and ligation into the EcoRI–SalI sites of pEGFP-C3. pFLAG-CMV2-mLgl1 was provided by T. Pawson (Mount Sinai Hospital, Toronto, Toronto, Canada). pSUPERIOR-p32 shRNA was generated by ligating oligonucleotides 5′-GATCCCCGGATGAGAGTGACATCTTCTTCAAGAGAGAAGATGTCACTCTCATCCTTTTTC-3′ and 5′-TCGAGAAAAAGGATGAGAGTGACATCTT CTCTCTTGAAGAAGATGTCACTCTCATCCGGG-3′ into the BglII–XhoI sites of pSUPERIOR-neo-GFP (Oligoengine). To construct pQE-Hakai (amino acids 1 – 190) and pMAL-Rac-WT, cDNAs were produced by PCR using pcDNA-FLAG-Hakai and pRK5-myc-Rac-WT and inserted into a SmaI site of pQE and pMAL, respectively.

Antibodies

We used mouse anti-p32 antibody (ab24734; Abcam) for all immunoprecipitations and for Western blotting in Fig. 1 B, Fig. 2 (A, C, and D), Fig. S1 A, and Fig. S2 A. We also used mouse anti-p32 (clone 20; for Western blotting in Fig. S3, A and C; BD Biosciences), as well as rabbit anti-p32 (for Western blotting in Fig. 2 B and all immunofluorescence; Affinity BioReagents, Inc.). Mouse anti-FLAG antibody (M2) and horseradish peroxidase–conjugated mouse anti-FLAG antibody (M2; used for Western blotting in Fig. S1 E) were obtained from Sigma-Aldrich. Rabbit anti-MBP antibody and mouse anti-Myc (4A6) antibody (used for all immunoprecipitations and for Western blotting in Fig. 1 A [bottom blots] and Fig. S1, B and D) were purchased from New England Biolabs, Inc., and Upstate Biotechnology, respectively. Horseradish peroxidase–conjugated mouse anti-Myc (4A6) antibody (used for Western blotting in Fig. S2 E) was obtained from Upstate Biotechnology. Rabbit anti-Myc antibody used for Western blotting in Fig. 1 A (top) and Fig. S1 (B and C), was purchased from Santa Cruz Biotechnology, Inc. We used mouse anti-GFP antibody from Roche Diagnostics (7.1 + 13.1; for immunoprecipitation in Fig. 1 A, for Western blotting in Fig. 1 A [top four blots], Fig. 1 D, and Fig. S1 B, and for immunostaining in Fig. 4). Rabbit anti-GFP from Abcam (ab290) was used for Western blotting in Fig. 1 A (bottom four blots) and Fig. S1 F. The rabbit anti-PKCζ antibody (C-20) was obtained from Santa Cruz Biotechnology, Inc. To detect mLgl2 by Western blotting and immunofluorescence, we used mouse anti-Llgl2 (clone 4G2) from Abnova. We produced rabbit anti-mLgl2 polyclonal antibody against the peptide LRTGHDPARERLKRDLFQFC (Genosphere Biotechnologies), which was used for immunoprecipitation. To detect phosphorylated mLgl2, we used rabbit anti–mLgl2-S653P-2 antibody (provided by S. Ohno, Yokohama City University, Yokohama, Japan). Antibodies against E-cadherin (rat ECCD2) and ZO-1 (rabbit) were obtained from Zymed Laboratories. Rat anti–α-tubulin antibody (ab6161) was obtained from Abcam. Mouse anti–β-catenin antibody (clone 14) was obtained from BD Biosciences. Secondary antibodies used for the Licor Odyssey system were goat anti-mouse ALEXA 680 (Invitrogen) and goat anti-rabbit IRDye 800 (Li-Cor Biosciences).

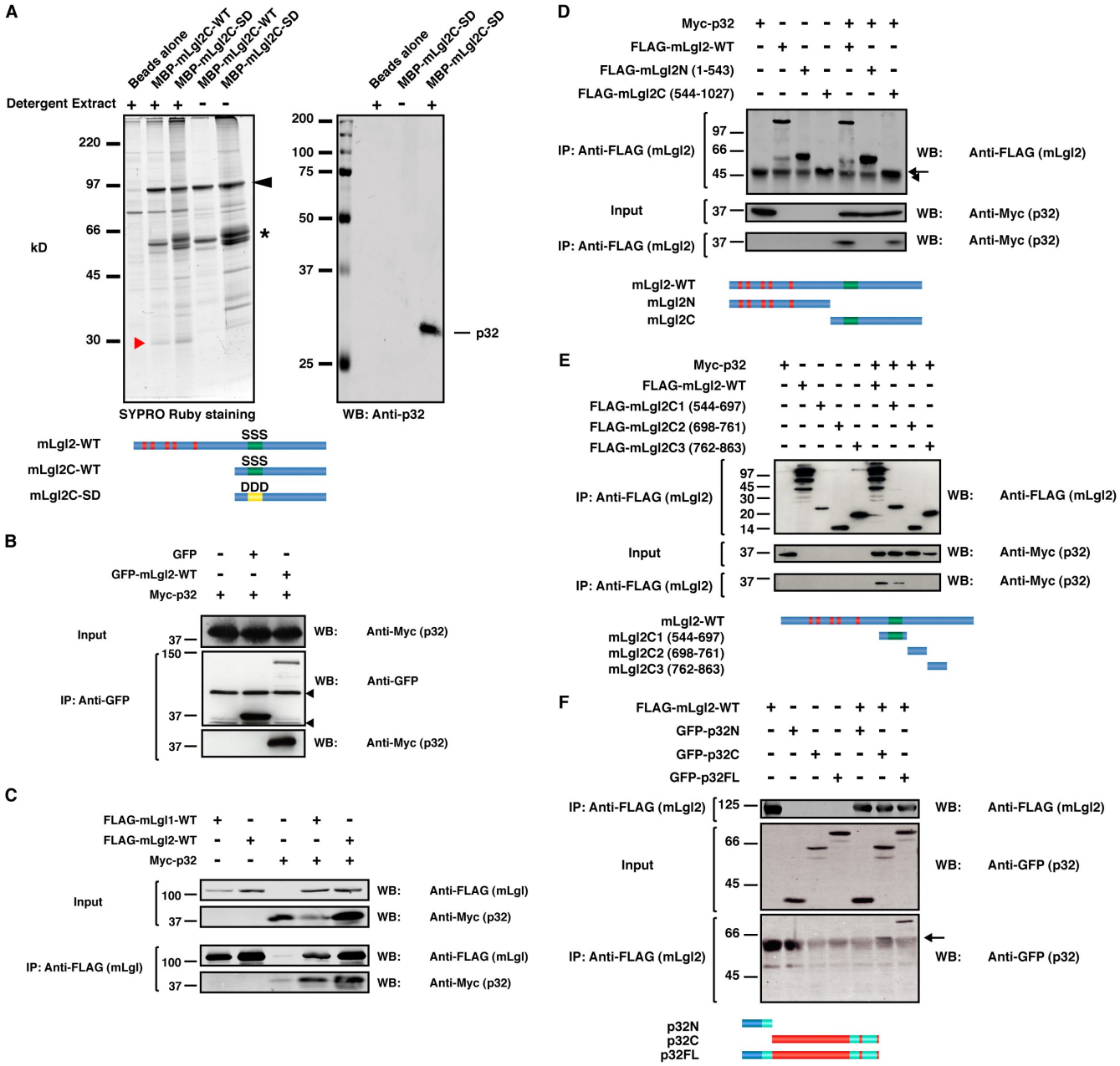

Figure S1. **Characterization of the interaction between mLgl2 and p32.** (A) Affinity purification of mLgl2 binding proteins from a detergent soluble fraction of rat kidney lysates using MBP-mLgl2C-WT and -SD coupled to amylose resin beads as bait. We generated two fusion proteins, MBP-mLgl2C-WT and MBP-mLgl2C-SD. In MBP-mLgl2C-SD, three serines of the aPKC phosphorylation site were changed to aspartic acid to generate a phosphomimetic mutant. Proteins bound to MBP-mLgl2C-WT and -SD were examined by SYPRO Ruby staining (left). The black arrowhead indicates MBP-mLgl2C proteins. The asterisk indicates degradation products of MBP-mLgl2C proteins. The red arrowhead indicates the protein band that was examined by mass spectrometric analysis. The identity of the mLgl2 binding protein was confirmed by Western blotting using anti-p32 antibody (right). The schematic illustrates the domain structures of mLgl2 and the truncated proteins used (red, WD40 domains; green, aPKC phosphorylation domain; yellow, aPKC phosphorylation domain with serines mutated to aspartic acid). (B) Specificity of the interaction between mLgl2 and p32. GFP-mLgl2-WT or GFP alone were coexpressed with Myc-p32 and immunoprecipitation was performed using anti-GFP antibody, followed by Western blotting using anti-GFP and anti-Myc antibodies. Arrowheads indicate the positions of the heavy and light chains of IgG. (C) Coimmunoprecipitation of mLgl1 and p32. FLAG-mLgl1 or mLgl2 was coexpressed with Myc-p32 in HEK293 cells, and immunoprecipitation was performed by using anti-FLAG antibody, followed by Western blotting with anti-FLAG and anti-Myc antibodies. (D) p32 binds to the C terminus of mLgl2. Full-length (FLAG-mLgl2-WT), N terminus (FLAG-mLgl2N), or C terminus (FLAG-mLgl2C) of mLgl2 were coexpressed with Myc-p32 in HEK293 cells. Immunoprecipitation was performed using anti-FLAG antibody, followed by Western blotting with anti-FLAG and anti-Myc antibodies. The arrow and arrowhead indicate the position of FLAG-mLgl2C and the heavy chain of IgG, respectively. (E) Coimmunoprecipitation of fragments of the C terminus of mLgl2 with p32. FLAG-tagged fragments of the C terminus of mLgl2 (FLAG-mLgl2C1, -2, or -3) and Myc-p32 were coexpressed in HEK293 cells. Immunoprecipitation was performed using anti-FLAG antibody, followed by Western blotting using horseradish peroxidase–conjugated anti-Myc and anti-FLAG antibodies. The most distal C-terminal fragment of mLgl2 (864–1027) was not analyzed because of low expression. (F) The C terminus of p32 is involved in the interaction with mLgl2. The full-length (GFP-p32FL), N terminus (GFP-p32N), or C terminus (GFP-p32C) of p32 was coexpressed with FLAG-mLgl2-WT in HEK293 cells. Immunoprecipitation was performed using anti-FLAG antibody, followed by Western blotting with anti-FLAG and anti-GFP antibodies. The arrow indicates the position of GFP-p32C. The schematic illustrates the p32 constructs used (blue, 73 amino acid precursor sequence; turquoise, α helices).

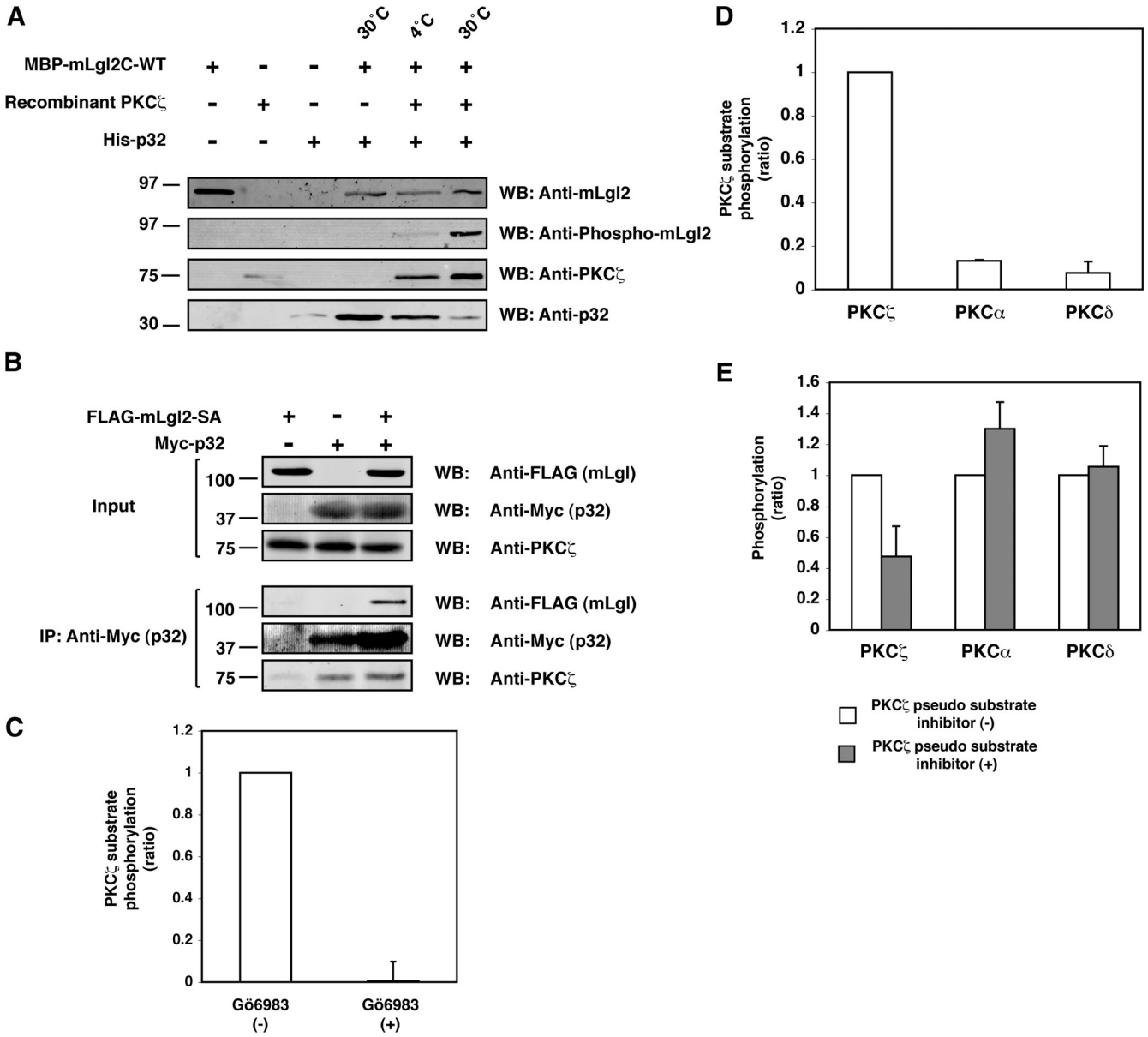

Figure S2. **p32 interacts with mLgl2 transiently and enhances PKCζ activity.** (A) MBP-mLgl2C-WT was incubated with PKCζ at 30 or 4°C, followed by incubation with His-p32 and pull-down assay using amylose resin beads. PKCζ and p32 bound to MBP-mLgl2C-WT were examined by Western blotting using anti-PKCζ and anti-p32 antibodies, respectively. The phosphorylation of mLgl2 was examined by Western blotting with anti–phospho-mLgl2 antibody. Together with Fig. 2 A, these data suggest that PKCζ enhances the interaction between mLgl2 and p32, but once mLgl2 is phosphorylated by PKCζ, p32 is no longer able to efficiently interact with the complex. In the absence of increased expression of PKCζ, MBP-mLgl2C-WT and the phosphomimetic mutant mLgl2C-SD interacted with equivalent amounts of p32 (Fig. S1 A, left), suggesting that the dissociation of p32 from mLgl2 may depend on PKCζ in the complex or that the mutation may not fully mimic phosphorylation. (B) The effect of overexpression of mLgl2 on the interaction between PKCζ and p32. FLAG-mLgl2-SA was coexpressed with Myc-p32 in HEK293 cells and immunoprecipitation was performed by using anti-Myc antibody, followed by Western blotting with anti-FLAG, anti-Myc, and anti-PKCζ antibodies. (C) Effect of a PKC inhibitor, Gö6983, on the phosphorylation of a PKCζ peptide substrate by p32 immunoprecipitate. Immunoprecipitation was performed from HEK293 cell lysates by using anti-p32 antibody or control IgG, followed by incubation of immunoprecipitates with PKCζ peptide substrate and γ-[^{32}P] ATP in the presence or absence of Gö6983. Peptide substrates were then collected by incubation with streptavidin beads, and the radioactivity of the beads was measured. The radioactive count by control IgG immunoprecipitate was subtracted from that by p32 immunoprecipitate, and results are expressed relative to the value in the absence of Gö6983 and represent the means ± SD of two independent experiments. (D) Specific phosphorylation of PKCζ peptide substrate by PKCζ. PKCζ peptide substrate was incubated in the same phosphorylation buffer as used in Fig. 2 C with γ-[^{32}P] ATP in the presence of 2 ng of recombinant PKCα, PKCδ, or PKCζ protein. Peptide substrates were then collected by incubation with streptavidin beads, and the radioactivity of the beads was measured. The radioactive count of streptavidin beads without PKCζ peptide substrate was subtracted from that with substrate. The results are expressed relative to the value in the presence of PKCζ and represent the means ± standard deviation of two to three independent experiments. (E) Effect of PKCζ pseudosubstrate inhibitor on phosphorylation by various PKCs. PKCζ pseudosubstrate inhibitor was added to a phosphorylation reaction with 100 ng of recombinant PKCα, PKCδ, or PKCζ protein. As a substrate, histone IIIs (200 ng) was used for PKCα and PKCδ, and MBP-mLgl2C (200 ng) was used for PKCζ. The radioactive count performed in the absence of PKC was subtracted from that with PKC. The reaction was duplicated per each experiment, and the results are expressed relative to the value in the absence of inhibitor for each PKC and represent the means ± SD of two independent experiments.

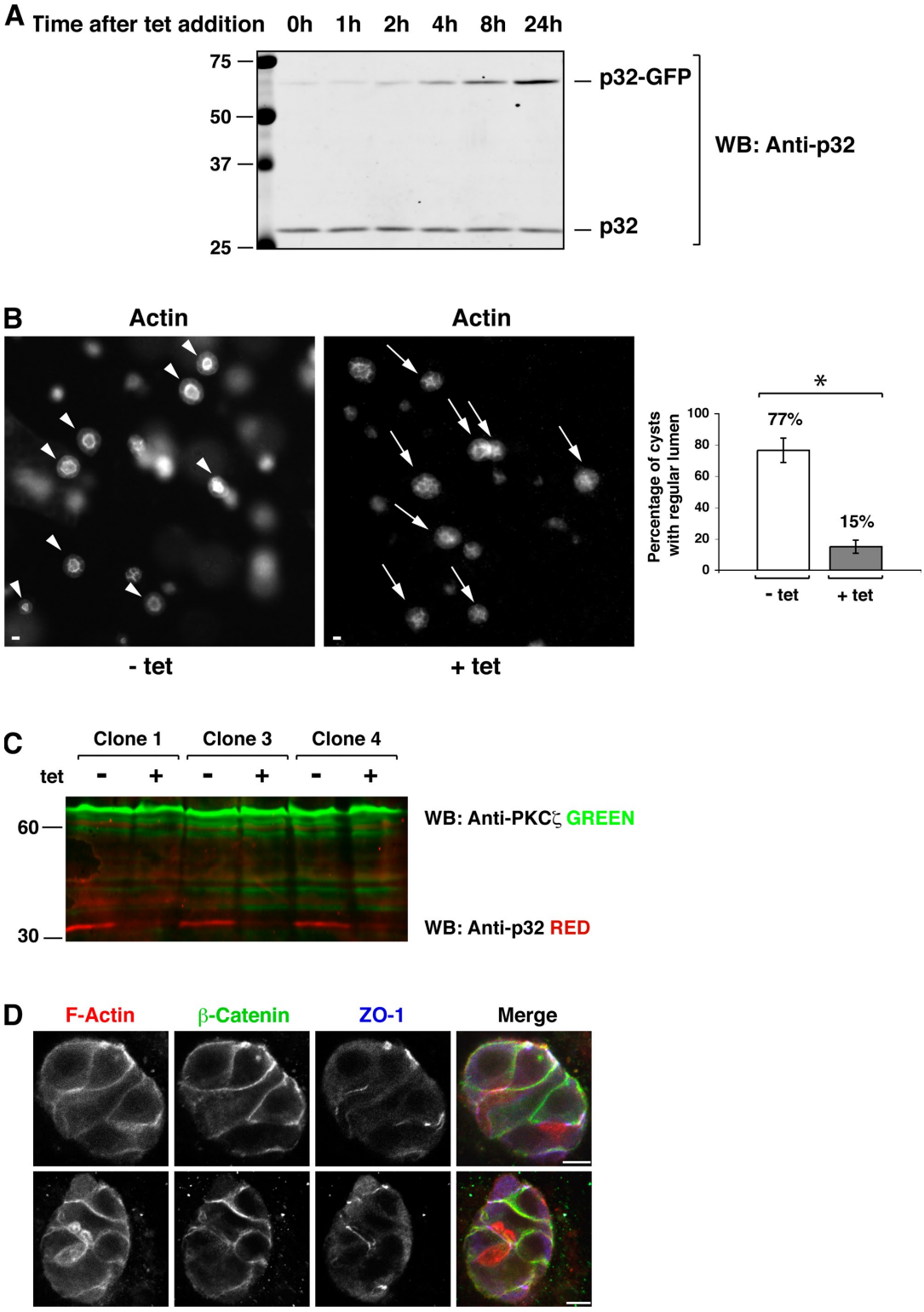

Figure S3. **p32 expression level affects cell polarity of MDCK cells in 3D culture.** (A) p32-GFP overexpression was induced in p32-GFP MDCK cells by addition of tetracycline, and cells were lysed at the indicated time points. The induction of p32-GFP expression was examined by Western blotting using anti-p32 antibody. p32-GFP was overexpressed ~1.5-fold at 24 h compared with endogenous p32. (B, left) Example images used for statistical analysis of cell polarity defects induced by p32 overexpression. Actin was stained using TRITC-phalloidin. White arrowheads indicate cysts with a regular lumen in noninduced MDCK cells. White arrows indicate cysts with an irregular lumen in p32-overexpressing MDCK cells. (right) Quantification of polarity defects in noninduced and p32-overexpressing MDCK cells. The percentage of cysts with actin enrichment and regular lumen formation was determined from two independent experiments ($n = 50$). *, $P < 0.015$. (C) Western blotting with anti-PKCζ and anti-p32 antibodies was performed using cell lysates from MDCK cell lines stably expressing p32 shRNA in a tetracycline-inducible manner cultured in the presence or absence of tetracycline. (D) Knockdown of p32 induces cell polarity defects in p32 shRNA–expressing MDCK cells. Immunostaining was performed using anti–β-catenin and anti–ZO-1 antibodies. Actin was visualized with TRITC-labeled phalloidin. Bars, 10 μm.